M-Shell Dielectronic Recombination: Theoretical Study

Sh. A. Abdel-Naby[1], D. Nikolić[1], T. W. Gorczyca[1],
N. R. Badnell[2], and D.W. Savin[3]

[1]Department of Physics, Western Michigan University, Kalamazoo MI 49008-5252, United States
[2]Department of Physics, University of Strathclyde, Glasgow G4 0NG, United Kingdom
[3]Columbia Astrophysics Laboratory, Columbia University, New York NY 10027, United States

Abstract. Dielectronic recombination (DR) is an important atomic physics process that is relevant to astrophysical plasma modeling. DR is responsible for the charge state balance as well as the cooling of plasmas, and it is the dominant electron-ion recombination process for most ions in both photoionized and collisionally-ionized plasmas. Accurate and reliable calculations for DR rate coefficients are needed to analyze the spectra obtained from astrophysical observations. Over the past few years, our group has computed reliable DR and radiative recombination (RR) data for all isoelectronic sequences up through Mg-like ions using a state-of-the-art multi-configuration Breit-Pauli (MCBP) approach. Recently, we have focused our work on the complex third-row M-shell isoelectronic sequences, especially Al-like. Although there exist some DR calculations for S^{3+}, those calculations were performed only within a non-relativistic LS-coupling approximation and for electron-ionized, higher temperatures. Fe^{13+} DR calculations have been completed and tested against the Heidelberg heavy-ion Test Storage Ring facility measurements. Semi-relativistic DR cross section and rate coefficient calculations for Al-like S^{3+} using the level-resolved distorted-wave AUTOSTRUCTURE program will be presented. The effect of ground-state fine structure on the DR rates will be discussed. These calculations include final-state-resolved partial DR and RR rate coefficients from the initial ground and metastable levels spanning a temperature range of $10\ z^2$ K - $10^7\ z^2$ K, where z is the initial ionic charge. Our computed Maxwellian DR rate coefficients are fitted into a simple formula for efficient dissemination of data and ease of use in plasma modeling codes, and comparisons to existing data will be shown.

Keywords: Dielectronic recombination, doubly-excited states.
PACS: 31.10.+z, 32.80.Dz, 34.80.Lx

INTRODUCTION

There has been much interest in measuring the oxygen-to-sulfur ratio in Jupiter's plasma torus [1]. Calculations for total DR rate coefficients for all sulfur ions were done with an application to magnetic fusion plasma in mind, in which a single-configuration approximation to calculate energies and transition rates was employed. Also, a cutoff on the number of states was applied [2]. DR rate coefficients for S^{q+} (q=1-5) ions have been calculated in the low density limit over the temperature range $T = 3\times10^4 - 10^6$ K that is applicable to the Io plasma torus [3]. Cross sections and rate coefficients for S^{3+} have been done using single-configuration and non-relativistic Hartree-Fock wave functions [4]. Photoionization cross sections and electron-ion recombination rate coefficients for S^{3+} were calculated in the close coupling approximation using the R-matrix method [5]. Other DR calculations were done for S^{3+} [6, 7]. All of these previous calculations for S^{3+} were performed only within a non-relativistic LS-coupling approximation and at higher temperatures more suitable for collisionally-ionized plasmas but not at the lower temperatures appropriate for photoionized plasmas. Our calculations include both LS and intermediate coupling (IC) approximations. MCBP cross sections and rate coefficients are computed using the AUTOSTRUCTURE suite of atomic structure and collision codes. The rest of the paper is organized as follows. The theoretical method is presented in Section 2, our results are presented in Section 3, and we follow with a brief summary.

METHODOLOGY

In order to study the dominant DR contributions, we consider an initial electron-ion collision state of a free electron incident on a S^{3+} ion which then undergoes radiationless capture into a doubly-excited

CP1099, *Application of Accelerators in Research and Industry: 20th International Conference*
edited by F. D. McDaniel and B. L. Doyle

resonance state, with a rate proportional, via the principle of detailed balance, to the reverse auoionization rate A_{a1}, followed by radiative decay to a final bound-state of S^{2+}, with radiative rate A_r, which can be schematically represented, for $\Delta n = 0$ core-excitations, as follows:

$$\begin{array}{ccc} & & S^{2+}(3\ell_1^2 3\ell_2 3\ell_3) + h\nu \\ & & \uparrow A_r \\ e^- + S^{3+}(3s^2 3p) & \xleftrightarrow{A_{a1}} & S^{2+}(3\ell_1 3\ell_2 3\ell_3 n\ell) \\ & & \downarrow A_r \\ e^- + S^{3+}(3\ell_1 3\ell_2^2) & \xleftarrow{A_{ai}} & S^{2+}(3\ell_1^2 3\ell_2 n\ell) + h\nu. \end{array} \quad (1)$$

Here ℓ_1, ℓ_2, and ℓ_3 take values from 0 to 2 (s, p, and d waves) and a neon closed core is assumed in all cases. The energy-averaged DR cross section is proportional to the autoionization rate A_{a1} multiplied by the branching ratio for radiative decay, with rate A_r, versus autoionization to either the ground or excited continua (with rates A_{a1} and $\sum_{i=2}^{n_0} A_{ai}$, respectively):

$$\langle\sigma\rangle \propto A_{a1} \frac{A_r}{A_r + A_{a1} + \sum_{i=2}^{n_0} A_{ai}}. \quad (2)$$

Here n_0 is the number of open channels.

We have used the AUTOSTRUCTURE code to calculate energy levels and radiative and autoionization rates in LS- and IC- (MCBP) calculations using non-relativistic radial functions [8, 9]. The autoionization rates are calculated in the isolated resonance approximation using distorted waves. This enables the generation of final-state level-resolved and total DR rate coefficients in the independent processes approximation, i.e., we neglect interference between the RR and DR processes [10]. In our calculation, n values were included up to 55 and a quantum-defect approximation for high-level values of n up to 1000 was used, while ℓ values were included up to 13.

The DR rate coefficient, as a function of temperature, from an initial ground or metastable state v to a final state i is given by

$$\alpha_{iv}^{z+1}(T) = \left(\frac{4\pi a_0^2 I_H}{k_B T}\right)^{3/2} \sum_j \frac{g_j}{2g_v} \exp(-\frac{E_c}{k_B T}) \times \frac{\sum_\ell A_{aj\to v,E_{c\ell}} A_{rj\to i}}{\sum_h A_{rj\to h} + \sum_{m,\ell} A_{aj\to m,E_{c\ell}}}, \quad (3)$$

where g_j is the statistical weight of the (N+1)-electron doubly-excited resonance state j, g_v is the statistical weight of the N-electron target state, and the autoionization rates , A_a, and radiative rates, A_r, are in inverse seconds. E_c is the energy of the continuum electron with angular momentum ℓ, which is fixed by the position of the resonance, I_H is the ionization potential energy of the hydrogen atom, k_B is the Boltzmann constant, and $(4\pi a_0^2)^{3/2} = 6.6011\times10^{-24}$ cm^3. For $\Delta n = 0$ core-excitation, the resonance energies are empirically adjusted so that the series limits match the $3\to3$ excitation energies obtained from the NIST database [11]. Accurate resonance energies are particularly important for the calculations of low-temperature DR rate coefficients. Our DR rate coefficient, $\alpha_v^{DR}(T)$, is fit to the following form:

$$\alpha_v^{DR}(T) = T^{-3/2} \sum_i c_i \exp(-\frac{E_i}{T}), \quad (4)$$

For RR we use the form [12]

$$\alpha_v^{RR}(T) = \frac{A\sqrt{T_0/T}}{(1+\sqrt{T/T_0})^{1-B}(1+\sqrt{T/T_1})^{1+B}}. \quad (5)$$

A more accurate representation, especially for low-charge ions, replaces B as [13]

$$B \to B + C\exp(-T_2/T). \quad (6)$$

RESULTS

Two different bases of configurations were used to describe the S^{3+} N-electron target system. This aids in assessing the accuracy of our calculations. Basis A consists of the $3s^23p$, $3s3p^2$, $3s^23d$, $3p^3$, $3s3p3d$, and $3p^23d$ configurations whereas basis B consists of basis A plus the $3s3d^2$ and $3p3d^2$ configurations. The (N+1)-electron configurations are then constructed by attaching an additional continuum or bound orbital to these configurations. Autoionization and (electric dipole) radiative rates are then determined from wave functions constructed using all such (N+1)-electron configurations, and these rates are used in Eq. (3) to produce the resultant DR cross sections. The radial wave functions are obtained by using the Slater-type-orbital model potential [14]. The 3s, 3p, and 3d radial scaling parameters, $\lambda_{n\ell}$, were determined by minimizing the equally-weighted sum of energies of the 40 lowest terms. A comparison between the calculated S^{3+} energy levels, the NIST values, and other available data [15-17], shown in Table 1, indicate basis B provides a better atomic structure description of S^{3+}. A further comparison of radiative transition rates, strength, for both bases, is given in Table 2.

TABLE 1. Energy levels (Ry) for S^{3+} using both bases compared to the NIST values [11].

Level	Configuration	Term	*J*	NIST	Basis A	Basis B
1	$3s^2 3p$	$^2P^o$	1/2	0.00000	0.00000	0.00000
2			3/2	0.00868	0.00745	0.00747
3	$3s3p^2$	^4P	1/2	0.64868	0.62075	0.61437
4			3/2	0.65182	0.62339	0.61701
5			5/2	0.65679	0.62766	0.62127
6	$3s3p^2$	^2D	3/2	0.85753	0.84936	0.84982
7			5/2	0.85796	0.84961	0.85007
8	$3s3p^2$	^2S	1/2	1.12550	1.23178	1.16091
9	$3s3p^2$	^2P	1/2	1.21763	1.25214	1.25414
10			3/2	1.22333	1.25635	1.25905
11	$3s^2 3d$	^2D	3/2	1.38634	1.45353	1.44717
12			5/2	1.38646	1.45368	1.44735
13	$3p^3$	^2D	3/2	1.68635	1.65870	1.65419
14			5/2	1.68719	1.65947	1.65496
15	$3p^3$	^4S	3/2	1.79023	1.81095	1.77213
16	3s3p3d	^4F	3/2	1.85391	1.83025	1.83183
17			5/2	1.85564	1.83176	1.83336
18			7/2	1.85813	1.83390	1.83550
19			9/2	1.86140	1.83668	1.83830
20	$3p^3$	^2P	3/2	1.92611	1.97556	1.94090
21			1/2	1.92620	1.97661	1.94158
22	3s3p3d	^4P	5/2	2.02482	2.01851	2.01467
23			3/2	2.02747	2.02056	2.01671
24			1/2	2.02932	2.02187	2.01802
25	3s3p3d	^4D	1/2	2.04436	2.05216	2.04325
26			3/2	2.04521	2.05278	2.04389
27			5/2	2.04615	2.05365	2.04476
28			7/2	2.04686	2.05460	2.04567
29	3s3p3d	^2D	5/2	2.12882	2.21248	2.14684
30			3/2	2.12910	2.21277	2.14706
31	3s3p3d	^2F	5/2	2.20204	2.27573	2.25591
32			7/2	2.20911	2.28181	2.26193
33	3s3p3d	^2P	3/2	2.41379	2.54315	2.51609
34			1/2	2.41536	2.54406	2.51778

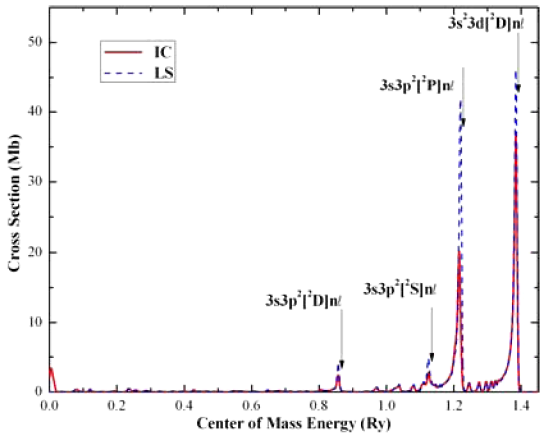

FIGURE 1. DR cross section of S^{3+} using both LS and IC coupling schemes, convoluted with a FWHM Gaussian of 0.1 eV for illustrative purposes, indicating that the dominant contribution to the Maxwellian-averaged rate coefficient comes from both $3s3p^2 n\ell$ and $3s^2 3d n\ell$ Rydberg series.

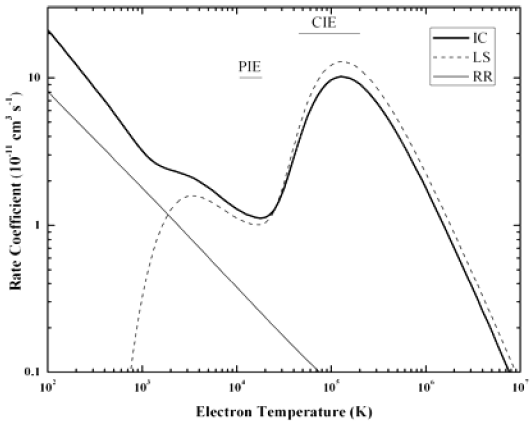

FIGURE 2. DR(IC), DR(LS) and RR rate coefficients of S^{3+} using both LS and IC-coupling schemes. PIE and CIE denote typical photoionization equilibrium and collisional ionization equilibrium [21].

A study of the DR cross section for S^{3+} in LS- and IC-coupling schemes reveals the dominant capture channel via $n = 3$ target core excitations. One can see from Fig. 1 that at higher energies the strongest contribution to the DR cross section, and therefore to the DR rate coefficient, comes from the $3p \rightarrow 3d$ excitation. Also, the calculated DR cross section for S^{3+} using IC-coupling is lower than the corresponding LS-coupling result. This is in contrast to the general IC vs LS trend [18, 19], where IC-coupling effects increase the number of resonances, and the resulting cross section, by roughly 50%. But this is for the case of a pure ground state such as Li-like ions ($1s^2 2s\ ^2S_{1/2}$). In our case, the ground state has a fine-structure splitting ($3s^2 3p\ ^2P_{1/2, 3/2}$) of around 0.118 eV.

The present *reduction* in the IC DR cross section is manifested in the DR rate coefficient, particularly in higher electron temperatures (see Fig. 2). At lower energies, the reason that the rate coefficient is higher using IC-coupling is due to additional contributions from the $3s^2 3p[^2P_{3/2}]n\ell$ core-excited resonance that are forbidden in LS-coupling, and more additional core-excited autoionizing states are opened up. The RR calculations are also shown in Fig.2.

TABLE 2. Summary of the most important radiative transition data, A_r, the line strengths, S, the oscillator strengths, f_L (length gauge) and f_V (velocity gauge). The superscripts mean that the whole line is corresponding to that source or basis.

Transition	A_r (10^9 s^{-1})	S (a.u.)	f_L	f_V
$3s3p^2\ ^2P_{1/2} \rightarrow 3s^2 3p\ ^2P_{1/2}$	4.854	1.847	0.385	0.385[a]
	5.911	2.238	0.468	0.468[b]
	5.691		0.477	0.490[c]
	5.720		0.478	0.485[d]
	5.463		0.456	0.456[e]
$3s3p^2\ ^2P_{3/2} \rightarrow 3s^2 3p\ ^2P_{1/2}$	1.587	1.196	0.250	0.250[a]
	1.591	1.191	0.250	0.250[b]
	1.549		0.257	0.263[c]
	1.554		0.257	0.260[d]
	1.494		0.249	0.249[e]
$3s^2 3d\ ^2D_{3/2} \rightarrow 3s^2 3p\ ^2P_{1/2}$	9.906	4.819	1.167	1.167[a]
	9.550	4.708	1.135	1.135[b]
	9.063		1.170	1.180[c]
	9.157		1.170	1.175[d]
	8.692		1.126	1.126[e]
$3s3p^2\ ^2P_{1/2} \rightarrow 3s^2 3p\ ^2P_{3/2}$	4.035	1.563	0.162	0.162[a]
	3.244	1.250	0.130	0.130[b]
	3.154		0.134	0.138[c]
	3.157		0.134	0.137[d]
	3.063		0.131	0.131[e]
$3s3p^2\ ^2P_{3/2} \rightarrow 3s^2 3p\ ^2P_{3/2}$	7.575	5.810	0.605	0.605[a]
	7.605	5.795	0.604	0.604[b]
	7.351		0.619	0.633[c]
	7.368		0.618	0.629[d]
	7.073		0.597	0.597[e]
$3s^2 3d\ ^2D_{3/2} \rightarrow 3s^2 3p\ ^2P_{3/2}$	2.034	1.005	0.121	0.121[a]
	1.961	0.982	0.118	0.118[b]
	1.879		0.123	0.124[c]
	1.891		0.122	0.123[d]
	1.801		0.118	0.118[e]
$3s^2 3d\ ^2D_{5/2} \rightarrow 3s^2 3p\ ^2P_{3/2}$	11.780	8.728	1.052	1.052[a]
	11.360	8.526	1.023	1.023[b]
	10.790		1.060	1.070[c]
	10.900		1.057	1.070[d]
	10.340		1.018	1.018[e]

[a] Basis A, [b] Basis B, [c] [15], [d] [16], and [e] [17]

In an attempt to understand the suppression of the DR cross section in IC-coupling, calculations were carried out for the $3s \rightarrow 3p$ excitation ($e^- + 3s^2 3p\ [^2P_{1/2}] \rightarrow 3s3p^2\ [^2P_{1/2, 3/2}]n\ell$). The resulting DR cross sections for both $3s3p^2\ [^2P_{1/2}, ^2P_{3/2}]n\ell$ series are convoluted with a full width at half maximum (FWHM) Gaussian of 1.2 meV (see Fig. 3). Both series begin to autoionize at principle quantum number $n = 31$. Also, the same calculations for the $3p \rightarrow 3d$ excitation ($e^- + 3s^2 3p\ [^2P_{1/2}] \rightarrow 3s^2 3d\ [^2D_{3/2, 5/2}]n\ell$) were studied, and the

resulting DR cross sections are plotted in Fig. 4. Again, the DR cross section drop occurs abruptly at n = 31. Thus, the reason for the reduction in the IC cross section is that the $3s3p^2n\ell$ and $3s^23dn\ell$ series autoionize to additional continua at n = 31 and above, decreasing the resultant radiative branching ratio in Eq. (3) [20].

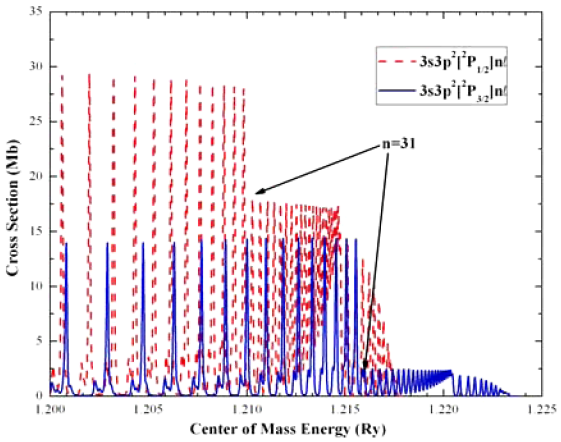

FIGURE 3. DR cross section for S^{3+} in IC-coupling for the collision $e^- + 3s^23p[^2P_{1/2}] \rightarrow 3s3p^2[^2P_{1/2},^2P_{3/2}]n\ell$, convoluted with a FWHM Gaussian of 1.2 meV. A sudden drop in the cross section occurs for both series at n = 31.

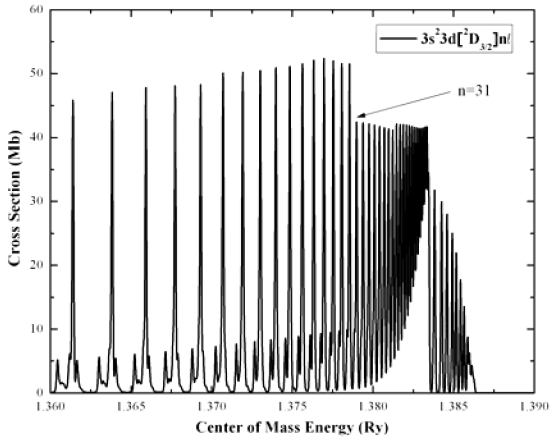

FIGURE 4. Same as Fig. 3 but for the collision $e^- + 3s^23p[^2P_{1/2}] \rightarrow 3s^23d[^2D_{3/2}]n\ell$.

In Fig. 5, we present comparisons between our calculated LS- and IC-coupling results and other available data for S^{3+} [3, 5-7]. In Tables 3 and 4, we present separately the fitting coefficients for our total DR and RR rate coefficients for the ground and metastable levels (indexed by m and referring to those listed in Table 1) , following forms given by Eqs (4) and (5), respectively. The fits are accurate to better than 3% over z^2 (10^1–10^7) K, where z = 3.

TABLE 3. DR fitting coefficients c_i ($cm^3\ s^{-1}\ K^{3/2}$) and E_i (K) for the ground and metastable initial levels (m = 1–5) of S^{3+}. The m-values are referring to those listed in Table 1.

m	c_1	c_2	c_3	c_4	c_5	c_6	c_7	c_8	c_9	c_{10}	c_{11}
1	3.437(-7)	1.029(-6)	3.374(-5)	5.382(-4)	5.382(-4)	3.546(-3)	3.546(-3)	3.546(-3)	3.547(-3)	3.547(-3)	6.165(-5)
2	5.494(-7)	7.527(-6)	1.473(-4)	1.863(-3)	2.533(-3)	2.532(-3)	2.532(-3)	2.532(-3)	2.532(-3)	4.610(-5)	
3	1.417(-8)	2.589(-7)	2.327(-6)	4.397(-6)	5.639(-5)	6.467(-5)	1.092(-4)	1.092(-4)	1.074(-4)	3.205(-7)	
4	1.626(-8)	2.541(-6)	1.672(-6)	4.397(-6)	6.132(-5)	1.019(-4)	9.519(-5)	9.432(-5)	9.429(-5)	1.634(-6)	
5	1.297(-6)	1.792(-6)	5.444(-6)	5.686(-5)	6.249(-5)	5.473(-5)	6.123(-5)	6.277(-5)	6.289(-5)	6.302(-5)	
m	E_1	E_2	E_3	E_4	E_5	E_6	E_7	E_8	E_9	E_{10}	E_{11}
1	5.767(1)	5.524(2)	1.395(4)	8.289(4)	2.033(5)	2.033(5)	2.033(5)	2.033(5)	2.033(5)	2.033(5)	1.103(6)
2	4.017(3)	6.733(3)	3.890(4)	1.489(5)	2.004(5)	2.010(5)	2.010(5)	2.017(5)	2.017(5)	9.936(5)	
3	1.061(2)	4.033(2)	1.431(3)	8.085(3)	2.413(4)	4.207(4)	8.890(4)	8.890(4)	1.297(5)	1.412(6)	
4	1.675(2)	7.393(2)	2.030(3)	8.685(3)	2.411(4)	5.467(4)	1.073(5)	1.073(5)	1.073(5)	9.534(5)	
5	1.524(2)	5.866(2)	7.694(3)	2.399(4)	5.839(4)	5.839(4)	1.085(5)	1.085(5)	1.085(5)	1.085(5)	

TABLE 4. RR fitting coefficients for the ground and metastable initial levels (m=1-5) of S^{3+}.

m	A ($cm^3\ s^{-1}$)	B	T_0(K)	T_1(K)	C	T_2(K)
1	2.035(-10)	0.6345	3.158(1)	3.487(7)	0.0926	1.397(5)
2	4.748(-12)	0.4814	1.158(4)	2.940(7)	0.2676	1.164(5)
3	7.570(-12)	1.0388	3.570(2)	1.889(7)	0.0917	2.190(4)
4	7.425(-12)	1.0394	3.709(2)	1.858(7)	0.0921	2.188(4)
5	2.060(-11)	1.0288	4.712(1)	2.091(7)	0.0711	2.388(4)

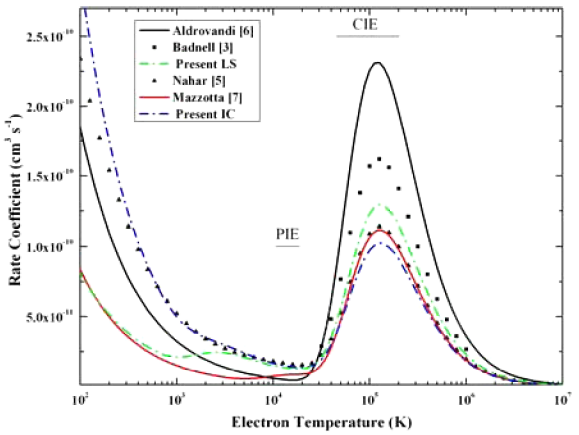

Figure 5. Comparisons between present and previously existing DR + RR rate coefficients for S^{3+} [3, 5-7].

SUMMARY

Our present investigation into the DR process of Al-like S^{3+} has revealed that a sufficiently large atomic configuration basis leads to fairly accurate energies and transition rates for the target levels, and should yield reliable DR cross sections. With the inclusion of IC-coupling effects, additional radiatively-decayed states can autoionize, thereby decreasing the DR cross section. This occurs near the Rydberg limits and reduces the high-temperature rate coefficient that is more important for collisionally-ionized plasmas. On the other hand, IC effects open up additional core-excited autoionizing states, thereby increasing the low-energy DR cross section. This leads to a substantial increase in the low-temperature rate coefficient that is important for photoionzed plasmas. These findings are a reminder that, as usually is the case, relativistic (i.e., spin-orbit) effects can have a profound effects even for low ionization stages for low-charge ions. Despite the relative weakness of spin-orbit effects, which scale as z^4 and are expected to be least important for low ionization stages such as the present case of S^{3+}, even small energy shifts create additional autoionizing levels that greatly affect the resulting rate coefficient.

ACKNOWLEDGMENTS

This work was supported in part by NASA APRA and SHP SR&T programs.

REFERENCES

1. D. E. Shemansky, J. Geophys. Res. **92**, 6141 (1988).
2. V. L. Jacobs, J. Davis, J. E. Rogerson, and M. Blaha, Astrophys. J **230**, 627 (1979).
3. N. R. Badnell, Astrophys. J. **379**, 375 (1991).
4. A. Al-Mulhem and I. Nasser, Phys. Rev. A **46**, 2945 (1992).
5. S. N. Nahar, Astrophys. J. Suppl. Ser. **126**, 537 (2000).
6. S. M. V. Aldrovandi and P. Pequignot, A&A **25**, 137 (1973).
7. P. Mazotta, G. Mazzitelli, S. Colafrancesco, and N. Vittorio, Astron. Astrophys. Suppl. Ser. **133**, 403 (1998).
8. N. R. Badnell, J. Phys. B **19**, 3827 (1987).
9. N. R. Badnell, J. Phys. B **30**, 1 (1997).
10. M. S. Pindzola, N. R. Badnell, and D. C. Griffin, Phys. Rev. A **46**, 5725 (1992).
11. http://physics.nist.gov/asd3.
12. D. A. Verner and G. J. Ferland, Astrophys. J. Suppl. Ser. **103**, 467 (1999).
13. M. F. Gu, Astrophys. J. **590**, 1131 (2003).
14. A. Burgess, H. E. Mason, and J. A. Tully, Astron. Astrophys. **217**, 319 (1989).
15. S. S. Tayal, J. Phys. B **32**, 5311 (1999).
16. G. P. Gupta and A. Z. Msezane, J. Suppl. Ser. **130**, 227 (2000).
17. A. Hibbert, T. Brage, and J. Fleming, Mon. Not. R. Astron. Soc. **333**, 885 (2002).
18. E. J. Trefftz, in *in Physics of The One and Two Electron Atoms*, edited by F. Bopp and H. Klein-poppen, North-Holand, Amsterdam, 1969, pp. 839.
19. D. C. Griffin, M. S. Pindzola, and C. Bottcher, Phys. Rev. A **31**, 568 (1985).
20. M. Blaha, Astrophys. Letters **10**, 179 (1972).
21. P. Bryans, E. Landi, and D. W. Savin, Astrophys. J, **in press**, [arXiv:0805.3302] (2008).